

BIFURCATION ANALYSIS OF SHALLOW SPHERICAL SHELLS WITH MERIDIONALLY NONUNIFORM LOADING

Charles G. Lange* & Frederic Y.M. Wan

Department of Mathematics

University of California, Irvine, CA92697-3875, U. S. A.

fwan@math.uci.edu

Abstract Numerical solutions of the relevant boundary value problem suggest that the first bifurcation from the basic solution for a spherical cap under a class of meridionally nonuniform loading is to a dimple state. Delicate asymptotic analysis of the linearized buckling problem confirm this observation.

1. Introduction

Under favorable conditions, dome-shaped, thin elastic shell of revolution is known to undergo a predominantly inextensional bending type deformation in the form of a finite axisymmetric dimple centered at the apex of the shells. The possibility of polar dimpling was suggested in [1] and investigated in [2-9] and elsewhere. Consider for example a very thin shallow clamped spherical cap subject to a quadratically varying pressure loading $p_n = p_o(1 - c^2x^2)$, where $x = r/r_o$ is the radial distance from the axis of revolution of the cap's middle surface normalized by its value at the outer edge. It was shown in [9] that polar dimpling is a possible mode of deformation if $c > 1$ and $p_o \geq p_{cr}$ for some critical load magnitude p_{cr} . Moreover, for very thin shells, we see from the results of [9] that p_{cr} is much smaller than the classical buckling load for a complete spherical shell p_s with the same radius of curvature, i.e., $p_{cr} \ll p_s$. This gives rise to the possibility of axisymmetric buckling at

*Deceased

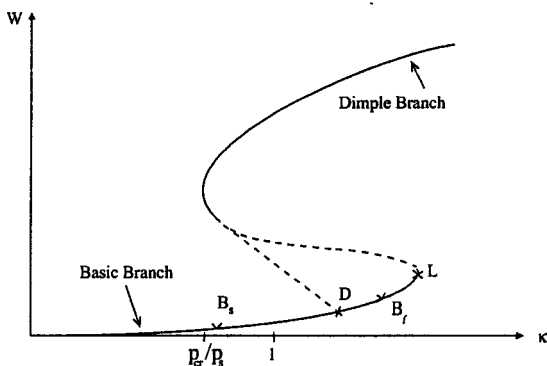


Figure 8.1. LOAD DEFORMATION CURVE

load level comparable to, or well below the critical load for unsymmetrical buckling. An investigation of axisymmetric buckling for meridionally nonuniform pressure loading is therefore of interest.

With $p_o = p_{cr}$, the size of the resulting dimple was found in [9] to be given by the dimensionless dimple (base) radius $x_{cr} = \sqrt{2/3}c^{-1}$. For larger values of p_o , two dimples of different sizes are possible, one with dimensionless dimple radius $x_G > x_{cr}$ and the other with dimensionless dimple radius $x_L < x_{cr}$. As p_o increases, x_G increases toward unity or $x_t = \sqrt{2}/c$ whichever is smaller, while x_L decreases to zero. Whether the dimple mode is possible or not, a non-dimple mode of deformation (called the basic branch hereafter) is also possible up to a certain threshold load magnitude. (A more precise description will be given later.) These results may be summarized by an overall load-deformation plot such as the one shown in Figure 8.1 giving the L_2 norm, W , of the axial displacement of the shell's midsurface as a function of a dimensionless load magnitude parameter $\kappa = p_o/p_s$. Accurate numerical solutions of the relevant nonlinear boundary value problem governing the elastostatics of the spherical cap give the solid curves in Figure 8.1 as (a qualitative description of) the overall load-deformation relation corresponding to a typical load-geometric configuration. The qualitative features of the shell behavior described above for a spherical cap subject to a particular pressure distribution are typical for many dome-shaped thin elastic shells of revolution subject to more general axisymmetric loading. They give rise to several questions which are important in design studies: Is the *dimple branch* of the load-deformation relation in Figure (1) the result of a bifurcation from the basic branch at some point D , or the consequence of the presence of a limit point L along an S shape load-

deformation curve as indicated by the dotted portion connecting the top of the basic branch to the dimple branch? Does bifurcation (buckling) occur elsewhere along the basic branch, e.g., at some B_ℓ and B_s ? Is the buckling load above (as in the case of B_ℓ) or below (as in the case of B_s) p_s ? The answers to these important questions for the specific problem of a spherical cap as well as similar questions for other dome-shaped thin shells of revolution with more general axisymmetric loading evidently cannot be obtained from numerical solutions of the relevant boundary value problems, however accurate these solutions may be. In this paper, we show that it is possible to gain some insight to the actual shell behavior by obtaining asymptotic solutions of the relevant boundary value problems and eigenvalue problems. For simplicity, we consider here only the spherical cap problem and obtain an asymptotic solution for the basic branch behavior and for the *axisymmetric* buckling load of the "linearized" buckling theory. The basic mathematical problem in our axisymmetric buckling analysis is an eigenvalue problem which is nonlinear in the eigenvalue parameter. It is of some mathematical interest that a matched asymptotic solution of this eigenvalue problem requires an intermediate layer solution to connect the inner solution near the apex of the shell to a WKB type solution away from the apex. To the authors, the presence of such an intermediate layer solution is novel and rather unexpected.

2. Formulation

Consider an elastic shell of revolution which has undergone infinitesimal strain, and axisymmetric finite deformations. The elastostatics of such a shell may be formulated as a boundary value problem for two simultaneous second order nonlinear ordinary differential equations for a stress function and a meridional slope variable [10,11]. For a shallow spherical cap with an undeformed meridional slope $\xi_0 x$, subject to a normal¹ pressure distribution $p_n = p_0 p(x)$ where p_0 is chosen so that $p(x) \leq 1$, we may take these equations in the following dimensionless form [11]:

$$\epsilon^2 x [\Psi'' + \frac{1}{x} \Psi' - \frac{1}{x^2} \Psi] + \frac{1}{2} (\Phi^2 - x^2) = 0 \quad (2.1)$$

$$(0 < x < 1)$$

$$\epsilon^2 x [\Phi'' + \frac{1}{x} \Phi' - \frac{1}{x^2} \Phi] - \Phi \Psi = 4\kappa x P(x) \quad (2.2)$$

with

$$P(x) = \frac{1}{x} \int_0^x p(t) t dt. \quad (2.3)$$

In (2.1)-(2.3), a prime indicates differentiation with respect to the dimensionless radial coordinate x (as defined in section (1)) and $\xi_0 \Phi(x)$ denotes the meridional slope of the deformed middle surface of the shell. In terms of radial coordinate r_0 of the shell edge, the shell thickness h , Young's modulus E and Poisson's ratio ν , we also

$$\varepsilon^2 = \frac{ha}{2r_0^2 \sqrt{3(1-\nu^2)}}, \quad \kappa = \frac{p_0}{p_s}, \quad p_s = \frac{2Eh^2}{a^2 \sqrt{3(1-\nu^2)}} \quad (2.4)$$

where $a = r_0/\xi_0$ is the radius of the spherical middle surface and p_s is the classical buckling load of a complete spherical shell under uniform pressure. The dimensionless stress function Ψ is the conventional stress function normalized by $p_s a r_0/4$ with $p_s a \Psi/4x$ and $p_s a \Psi'/4$ being the radial and hoop stress resultant of the shell, respectively.

The fourth order system of the two ODE, (2.1)-(2.2), is supplemented by four boundary conditions. Two are regularity conditions at the apex of the shell:

$$x = 0 : \quad \Phi = 0, \quad \Psi = 0, \quad (2.5)$$

(with the second being a consequence of the symmetry condition of no radial displacement at the apex). The other two come from the edge constraints at $x = 1$. For a clamped edge, we have

$$x = 1 : \quad \Phi = 1, \quad \Psi' - \nu \Psi = 0. \quad (2.6)$$

They correspond to the condition of no change in meridional slope and no radial displacement at the edge.

With $H = r_0^2/2a$ being the rise of the shell edge above the base plane tangent to the apex, the parameter $\varepsilon^2 = O(h/H)$ is a measure of the thickness-to-rise ratio. In this paper, we consider only the range $\varepsilon^2 \ll 1$ so that the spherical cap behaves as a shell (rather than a flat plate). We will also focus our discussion on the case of a quadratically varying normal load with

$$p(x) = 1 - c^2 x^2, \quad P(x) = \frac{1}{2} x \left(1 - \frac{1}{2} c^2 x^2 \right). \quad (2.7)$$

It should be clear from the subsequent development that a similar analysis may be carried out for other loadings and edge supports.

3. The Basic Branch Solution

It is not difficult to see that the system (2.1) and (2.2) with $P(x)$ given by (2.7) has an exact solution

$$\Phi_p = Ax, \quad \Psi_p = \frac{\kappa}{A}x(c^2x^2 - 2) \tag{3.1}$$

where A is a root of

$$A^3 - A + 16\varepsilon^2c^2\kappa = 0 \tag{3.2}$$

The cubic equation has only one negative root if $16\varepsilon^2c^2\kappa > 2/(3\sqrt{3})$ or $\kappa > \kappa_T \equiv [24\sqrt{3}c^2\varepsilon^2]^{-1}$, one negative and one positive (double) root if $\kappa = \kappa_T$, and one negative and two positive roots if $0 < \kappa < \kappa_T$. For $0 < 16\varepsilon^2c^2\kappa \ll 1$, the three roots may be obtained in the form of parametric series in powers of ε^2 :

$$A = \begin{cases} 1 - 8\kappa c^2\varepsilon^2 + \dots \equiv A_b \\ -1 - 8\kappa c^2\varepsilon^2 + \dots \equiv A_d \\ 16\kappa c^2\varepsilon^2[1 + (16\kappa c^2\varepsilon^2)^2 + \dots] \equiv A_f \end{cases} \tag{3.3}$$

Note that the larger positive root is slightly less than unity, the smaller positive root is slightly larger than zero and the negative root is slightly less than -1 . For fixed values of c and ε , both A_b and A_d decrease while A_f increases with $\kappa (\geq 0)$.

The exact solution (3.1) of the ODE also satisfies the regularity conditions (2.5) at $x = 0$, but does not satisfy the clamped edge conditions (2.6) at $x = 1$. With $\varepsilon^2 \ll 1$, this exact solution of (2.1), (2.2) and (2.5) may be modified by a boundary layer correction so that the modified solution also satisfies the clamped edge conditions (2.6) asymptotically and therefore is an asymptotic solution of the boundary value problem for Φ and Ψ . We omit the routine calculations for the method of matched asymptotic expansions and merely give here the final composite basic branch solution, denoted by Φ_b and Ψ_b , corresponding to the root A_b of the cubic equation (3.2):

$$\Phi_b = A_b x + \frac{\kappa\varepsilon}{\lambda_p - \lambda_m} [(3 - \nu)c^2 - 2(1 - \nu)][e^{\lambda_p \bar{x}} - e^{\lambda_m \bar{x}}] + O(\varepsilon^2)$$

$$\begin{aligned} \Psi_b = & \frac{\kappa}{A_b} x(c^2x^2 - 2) + \frac{\kappa\varepsilon}{\lambda_p - \lambda_m} [(3 - \nu)c^2 - 2(1 - \nu)][(\lambda_p^2 - \bar{\kappa})e^{\lambda_p \bar{x}} \\ & - (\lambda_m^2 - \bar{\kappa})e^{\lambda_m \bar{x}}] + O(\varepsilon^2) \end{aligned} \tag{3.4}$$

where

$$\begin{aligned}\bar{x} &= \frac{1-x}{\varepsilon}, & \bar{\kappa} &= \frac{1}{2}\kappa(c^2-2) \\ \lambda_p &= -\sqrt{\bar{\kappa} + \sqrt{\bar{\kappa}^2 - 1}}, & \lambda_p^2 &= \bar{\kappa} + \sqrt{\bar{\kappa}^2 - 1} \\ \lambda_m &= -\sqrt{\bar{\kappa} - \sqrt{\bar{\kappa}^2 - 1}}, & \lambda_m^2 &= \bar{\kappa} - \sqrt{\bar{\kappa}^2 - 1}\end{aligned}\quad (3.5)$$

The matched asymptotic expansion solution (3.4) was obtained under the assumption $8\kappa c^2 \varepsilon^2 \ll 1$ and is therefore valid only for sufficiently small values of ε . To the same order of approximation, we may set $A_b = 1$ in (3.4).

The asymptotic solution (3.4) is also inappropriate when $\bar{\kappa}$ is nearly unity, say $\bar{\kappa} = 1 + O(\varepsilon)$, for we have $\lambda_p - \lambda_m = O(\varepsilon)$ at most in that case. It is not difficult to verify that an appropriate basic solution for $\bar{\kappa} = 1 + O(\varepsilon)$ is given by

$$\begin{aligned}\Phi_B &\sim A_b x - \varepsilon \left[2\bar{x} \left(\nu - \frac{3c^2 - 2}{c^2 - 2} \right) e^{-\bar{x}} \right] \\ \Psi_B &\sim \frac{\kappa x}{A_b} (c^2 x^2 - 2) + \varepsilon \left[(4 + 2\bar{x}) \left(\nu - \frac{3c^2 - 2}{c^2 - 2} \right) e^{-\bar{x}} \right]\end{aligned}\quad (3.6)$$

where A_b may be approximated by unity and

$$\kappa = \frac{2}{c^2 - 2} [1 + O(\varepsilon)].\quad (3.7)$$

Both the basic branch solution (3.5) for $\bar{\kappa}$ away from unity and the basic branch solution (3.6) for $\bar{\kappa} = 1 + O(\varepsilon)$ will be needed in the buckling analysis in a later section.

Numerical solutions for different combinations of c , ε and κ accurate to at least five significant figures have been generated by the general boundary value problem solver COLSYS (or COLNEW) [12, 13] to confirm the adequacy of the asymptotic solution (3.4) for $8\kappa c^2 \varepsilon^2 \ll 1$. The difference between the numerical and asymptotic solution is at most $O(16\kappa c^2 \varepsilon^2)$ in all cases. Beyond the range of parameter values allowed by the asymptotic solution (3.4), COLSYS has also been used to generate the basic branch solution as well as the corresponding portion of the overall load-deformation curve in Figure (1) for different combinations of $c (> 1)$ and $\varepsilon (<< 1)$ and for κ beyond the range $8\kappa c^2 \varepsilon^2 \ll 1$. We could not obtain a basic branch solution for $\kappa \geq \bar{\kappa}_T$ for some upper bound $\bar{\kappa}_T$ which depends on the value of c and ε . For $c = 2$, we found that COLSYS failed to converge for sufficiently large κ for $\varepsilon = 0.01, 0.04$ and

0.1 with the upper bound $\bar{\kappa}_T$ for each ε given in Table (1). The corresponding value of $\kappa_T \equiv [24\sqrt{3}c^2\varepsilon^2]^{-1}$ beyond which there cannot be a positive root for (3.2) (and hence not a basic branch solution) are also listed there for comparison.

Table (1) The Values of κ_T and $\bar{\kappa}_T$ for $c = 2$

ε	0.01	0.04	0.1
$\bar{\kappa}_T$	60	3.1	0.48
κ_T	60.14...	3.759...	0.6014...

Also, COLSYS encountered convergence difficulty for several κ values well below the bound $\bar{\kappa}_T$ ($< \kappa_T$ in all cases). It raises the possibility of multiple equilibrium states associated with a bifurcation phenomenon at those κ values. As we shall see in the next section, bifurcation into another axisymmetric equilibrium state does occur at these κ values.

4. Bifurcation from the Basic Branch Solution

Bifurcation from the basic branch solution occurs when there are more than one solution of the boundary value problem (2.1), (2.2), (2.5) and (2.6) in the neighborhood of the bifurcation point. Let ϕ and ψ be the deviation of a second solution

$$\Phi = \Phi_b + \phi, \quad \Psi = \Psi_b + \psi \quad (4.1)$$

from the basic branch solution Φ_b and Ψ_b , respectively. The boundary value problem for Φ and Ψ can then expressed in terms of ϕ and ψ as

$$\begin{aligned} \varepsilon^2[\phi'' + \frac{1}{x}\phi' - \frac{1}{x^2}\phi] - \Phi_b\psi - \Psi_b\phi &= \phi\psi \\ \varepsilon^2x[\psi'' + \frac{1}{x}\psi' - \frac{1}{x^2}\psi] + \Phi_b\phi &= -\frac{1}{2}\phi^2 \end{aligned} \quad (4.2)$$

with

$$x = 0 : \quad \phi = 0, \quad \psi = 0 \quad (4.3)$$

$$x = 1 : \quad \phi = 0, \quad \psi' - \nu\psi = 0 \quad (4.4)$$

The problem (4.2)-(4.4) is a nonlinear eigenvalue problem with κ as the eigenvalue parameter. Near the point of bifurcation, we expect $|\phi|$ and $|\psi|$ generally to be relatively small of higher order compared to the basic branch solution and the ODE (4.2) can be linearized. Upon omitting

the nonlinear terms on the right hand side of (4.2), we are left with the linearized eigenvalue problem

$$\varepsilon^2 x[u'' + \frac{1}{x}u' - \frac{1}{x^2}u] - \Phi_b v - \Psi_b u = 0 \quad (4.2')$$

$$\varepsilon^2 x[v'' + \frac{1}{x}v' - \frac{1}{x^2}v] + \Phi_b u = 0$$

with

$$x = 0 : \quad u = v = 0 \quad (4.3')$$

$$x = 1 : \quad u = v' - \nu v = 0 \quad (4.4')$$

Note that the eigenvalue parameter κ appears nonlinearly in the basic branch solution Φ_b and Ψ_b . For $8\kappa\varepsilon^2 c^2 \ll 1$, the rather complex dependence of Φ_b and Ψ_b on κ can be seen from the asymptotic solution (3.4) and (3.5).

With Φ_b and Ψ_b already determined from section (3), the solution of the nonlinear eigenvalue problem (4.2)-(4.4) or of the linearized eigenvalue problem (4.2')-(4.4') may be obtained by various approximate methods. We confine ourselves to obtaining an approximate solution of the linearized problem in this article by three different methods. The first method is to discretize the continuous eigenvalue problem by approximating it by its finite difference analogue. To leading order in ε , Φ_b and Ψ_b are linear in κ , the difference analogue is, to the same order in ε , a matrix eigenvalue problem. The eigenvalues for the (N x N) matrix problem provide an approximate solution for the first N eigenvalues of the continuous problem. A second method of solution (which does not require a leading term approximation for Φ_b and Ψ_b) consists of solving the boundary value problem (4.2')-(4.4') for a fixed κ with the boundary condition $\phi(1)=0$ replaced by $\phi'(0)=1$. Starting with $0 < \kappa \ll 1$, repeat the solution process for an increasing sequence of κ values and, for each κ , check for a change in the sign of $\phi(1)$ from the solution for the previous value of κ . For every sign change, there is an eigenvalue between two successive values of κ .

With either method, the approximate eigenvalues found may be made more accurate by finding a COLSYS solution of the inhomogeneous linearized boundary value problem defined by (4.2')-(4.4') and

$$\kappa' = 0, \quad \phi'(0) = 1 \quad (4.5)$$

with the additional boundary condition serving only to normalize the eigenfunctions. The approximate eigenvalues and eigenfunctions found by either of the above methods provide the initial guesses for the iteration scheme of COLSYS. In this way, two eigenvalues are found near unity (to

five significant figure accuracy) for $c = 2$; $\nu = 0.3$ and for two different values of ε ; they are recorded in Table (2).

Table (2) Eigenvalues for Linearized Buckling Theory for $c = 2$ & $\nu = 0.3$ by COLSYS

ε	κ_1	κ_2
0.04	0.96465...	0.98533...
0.01	0.993806...	1.0138

Accurate numerical solutions were also obtained by COLSYS for the dimple branch solutions [9]. It is significant that, for the same two values of ε , the smaller of the two dimples shrinks as κ increases from κ_{cr} and eventually disappear around $\kappa \simeq 1$. This suggests that the dimple branch solution actually bifurcates from the basic branch solution at the buckling load. Unfortunately, the eigenvalues obtained by COLSYS in Table (2) may or may not be the lowest eigenvalues of the linearized eigenvalue problem as the iterative solution scheme in COLSYS may have converged to these larger eigenvalues. To find the lowest branch point, we consider in the next section an asymptotic solution of the linearized eigenvalue problem. Away from the apex of the spherical cap, an adequate approximate solution of (4.2')-(4.4') for $\varepsilon \ll 1$ may be obtained by the WKBJ method. Such an asymptotic solution is not uniformly valid for $0 \leq x \leq 1$, and the regularity conditions at $x = 0$ cannot be applied to the WKBJ solution. It is necessary to obtain also an asymptotic solution valid in the neighborhood of $x = 0$. Such a solution would be matched to the WKBJ solution in an intermediate region and then the clamped edge conditions would be used to determine the eigenvalues and therefore the bifurcation points along the overall load-deformation curve of the basic branch solution [14].

~~WKB~~ X

For $\bar{\kappa}$ away from unity and $c = 2$, (so that $\bar{\kappa} = \kappa$) the above method gives the following condition for the admissible values of $\bar{\kappa}$ for a non-trivial solution for ϕ and ψ :

Greek κ

$$\left[\frac{A^2 - \kappa}{2A} \right]^{\frac{1}{2}} \sinh \left[\frac{1}{\varepsilon} \left(\frac{\kappa}{A} \right)^{\frac{1}{2}} \left\{ \sqrt{1 + \gamma} + \gamma \ln \left(\frac{1 + \sqrt{1 + \gamma}}{\sqrt{\gamma}} \right) \right\} \right] \quad (4.6)$$

$$= \left[\frac{A^2 + \kappa}{2A} \right]^{\frac{1}{2}} \sin \left[\frac{1}{\varepsilon} \left(\frac{\kappa}{A} \right)^{\frac{1}{2}} \left\{ \sqrt{\tau - 1} + \frac{1}{2} \tau \sin^{-1} \left(\frac{1}{\sqrt{\tau}} \right) - \frac{3}{2} \pi \right\} \right]$$

where

$$\gamma = \frac{A^2 - \kappa}{2A\kappa}, \quad \tau = \frac{A^2 + \kappa}{2A\kappa} \quad (4.7)$$

and A is a function of κ (and vice versa) by the cubic equation (3.2). For $0 < \varepsilon \ll 1$, the roots of (4.6) must be such that we have $A^2 \approx \kappa$ ($=\bar{\kappa}$ as we have taken $c = 2$ in (4.6) and (4.7)); otherwise the exponential growth of hyperbolic sine term on the left cannot be matched by the (at most) algebraic growth on the right. We therefore conclude that, for $0 < \varepsilon \ll 1$, the linearized eigenvalue problem (4.2')-(4.4') for the determination of bifurcation from the basic branch admits only the trivial solution unless $\kappa \approx A^2$. From (3.2), we have for $\kappa = A^2$ (and $c = 2$),

$$A_b = \sqrt{1 + (32\varepsilon^2)^2} - 32\varepsilon^2 \cong 1 - 32\varepsilon^2 + O(\varepsilon^4)$$

$$\kappa = A^2 = 1 + 2(32\varepsilon^2)^2 - 64\varepsilon^2 \sqrt{1 + (32\varepsilon^2)^2} \simeq 1 - 64\varepsilon^2 + O(\varepsilon^4)$$

It follows that, for $0 < \varepsilon \ll 1$ and $c = 2$, branching from the basic solution does not occur if the pressure magnitude p_0 is not nearly the classical buckling pressure p_s of the complete spherical shell, say $\kappa = 1 + O(\varepsilon)$.

We note that no conclusion on bifurcation in the range $\kappa = 1 + O(\varepsilon) \approx A^2$ can be drawn from (4.6)-(4.7) as they were obtained with Φ_B and Ψ_B taken from (3.4). This asymptotic solution for the basic branch is not valid for $\kappa = 1 + O(\varepsilon)$; we should use the expressions given by (3.6) instead. When we applied the same solution process with Φ_B and Ψ_B taken from (3.6), we found that it is not possible to match the WKBJ solution (valid away from $x = 0$) with the Bessel function solution (valid near the apex of the shell) for the linearized eigenvalue problem (4.2')-(4.4'). As we shall see in the next section, an χ intermediate layer solution is required to bridge the two solutions. χ an

5. Asymptotic Analysis of the Linearized Eigenvalue Problem

5.1 Bessel Function Solution Near the Apex

For $\varepsilon \ll 1$, an asymptotic solution of the linearized eigenvalue problem (4.2')-(4.4') is complicated by the singularity of the differential equations at $x = 0$. In the neighborhood of the apex of the cap, we set $y = x/\varepsilon$ and write the ODE(4.2') as

$$L_y[u] - [A_b + \chi(e^{-1/\varepsilon})]v + \frac{2\kappa}{A_b} \left[\left(1 - \frac{1}{2}C^2\varepsilon^2 y^2\right) + O(e^{-1/\varepsilon}) \right] u = 0 \quad (5.1)$$
 χ \mathcal{O}

$$L_y[v] + [A_b + O(e^{-1/\varepsilon})]u = 0$$

with

$$L_y[f] \equiv \frac{d^2 f}{dy^2} + \frac{1}{y} \frac{df}{dy} - \frac{1}{y^2} f \quad (5.2)$$

For the basic branch solution, we have $A_b = 1 + O(\kappa c^2 \varepsilon^2) = 1 + O(\varepsilon^2)$ as we consider in this section only $\kappa \approx A^2$. We also take $c = 2$ to simplify the discussion. In that case we have $\kappa = \bar{\kappa} = [1 + \alpha_1 \varepsilon + \alpha_2 \varepsilon^2 + \dots]$ and omit the exponentially small terms to simplify (5.1) to

$$L_y[u] - [1 + O(\varepsilon^2)]v + \frac{2[1 + \alpha_1 \varepsilon + O(\varepsilon^2)][1 - 2\varepsilon^2 y^2]}{[1 + O(\varepsilon^2)]}u = O(e^{-1/\varepsilon}) \quad (5.1')$$

$$L_y[v] + [1 + O(\varepsilon^2)]u = O(e^{-1/\varepsilon})$$

We may now (tentatively) consider a regular perturbation solution for u and v in powers of ε . The leading term u_0 and v_0 of this perturbation solution is of course given by

$$L_y[u_0] - v_0 + 2u_0 = 0 \quad (5.3)$$

$$L_y[v_0] + u_0 = 0$$

with the regularity conditions (see(4.3'))

$$x = 0 : \quad u_0(0) = v_0(0) = 0. \quad (5.4)$$

It is not difficult to verify that the exact solution of (5.3) and (5.4) is

$$v_0 = a_0 J_1(y) + b_0 y J_1^*(y), \quad (5.5)$$

$$u_0 = (a_0 + 2b_0) J_1(y) + b_0 y J_1^*(y)$$

where $(\)^* \equiv d(\)/dy$ and a_0 and b_0 are arbitrary real constants of integration to be determined by matching to an asymptotic solution for $x \gg \varepsilon$. For matching, we need the following asymptotic behavior of $J_1(y)$ and $yJ_1^*(y)$ for $y \gg 1$:

$$J_1(y) \sim \left(\frac{2}{\pi y}\right)^{\frac{1}{2}} \cos\left(y - \frac{3\pi}{4}\right) \{1 + O(y^{-3/2})\} \quad (5.6)$$

$$yJ_1^*(y) \sim -\left(\frac{2y}{\pi}\right)^{\frac{1}{2}} \sin\left(y - \frac{3\pi}{4}\right) \{1 + O(y^{-1/2})\}$$

5.2 WKBJ Solution Away from the Apex

Away from $x = 0$, an asymptotic solution of the linearized ODE (4.2') may be obtained by the standard WKBJ method. The solution process is complicated by the fact that the boundary layer terms in the basic branch solution Φ_b and Ψ_b (which appear as coefficients of the ODE for u and v) are no longer exponentially small near $x = 1$, and therefore cannot be neglected in the solution process. Fortunately, the contribution of

these boundary layer terms to the final WKB solution is nevertheless negligibly small (so that they can in fact be deleted from the ODE before the WKB calculations). We omit the details and simply write down the leading term WKB solution:

$$\begin{aligned} v &\sim c_0 e^{i[xs + \sin^{-1}x]/2\epsilon} e^{\frac{\alpha_1}{4}ixs/\sqrt{x(1-\frac{\alpha_1}{2})s(1-s^4)}} \\ &+ d_0 e^{-i[xs + \sin^{-1}x]/2\epsilon} e^{-\frac{\alpha_1}{4}ixs/\sqrt{x(1+\frac{\alpha_1}{2})s(1-s^4)}} \\ &+ (\text{complex conjugate of the two preceding terms}) \\ &\equiv v_0 + v_0^* \end{aligned}$$

$$u \sim s^2 v_0 + (s^2 v_0)^*$$

with

$$s = \sqrt{1-x^2} + ix, \quad 1-s^4 = 8x^2(1-x^2) + i4x(2x^2-1)\sqrt{1-x^2} \quad (5.7)$$

where c_0 and d_0 are arbitrary complex constants. For simplicity, we have given v and u in (5.7) only for the case $c = 2$ in the pressure distribution (2.7) for which extensive numerical results have been obtained and recorded in this article and elsewhere. We will henceforth focus our discussion on this case though a similar analysis applies to the general case.

Two of the four real constants in (5.7) may be determined by the two boundary conditions at $x = 1$. The remaining two constants are to be determined by matching the WKB solution with the Bessel function solution of section (5.1). However, for $x = z\delta_1(\epsilon)$ where $\delta_1(\epsilon) \rightarrow 0$ but $\delta_1(\epsilon)/\epsilon \rightarrow \infty$ as $\epsilon \rightarrow 0$, we have

$$v \sim \frac{c_0 i^{-3/2} e^{iz\delta_1/\epsilon - (\delta_1 z)^2/2\epsilon}}{2[\delta_1 z]^{1-\alpha_1/4}} [1 + O(z\delta_1)] \quad (5.7')$$

$$+ \frac{d_0 i^{-3/2} e^{-iz\delta_1/\epsilon + (\delta_1 z)^2/2\epsilon}}{2[\delta_1 z]^{1+\alpha_1/4}} [1 + O(z\delta_1)]$$

+ complex conjugate of the preceding terms

It is simply not possible to match v as given by (5.7') and v_0 as given by (5.5) with $y = z/\delta_0(\epsilon)$ where $\delta_0(\epsilon) \rightarrow 0$ as $\epsilon \rightarrow 0$, keeping in mind the asymptotic behavior of J_1 and J_1^* given by (5.6). This suggests an

intermediate layer solution exists to bridge the WKB solution and the Bessel function solution.

5.3 An Intermediate Layer Solution

The expression (5.7') for v must remain bounded for $x = O(\delta_1(\varepsilon))$. This suggests a stretched variable $z = x/\sqrt{\varepsilon}$ for the intermediate layer region. In terms of z , the ODE (4.2') may be written as

$$\varepsilon L_z[u] - [1 + O(\varepsilon^2)]v + \frac{2[1 + \alpha_1\varepsilon + O(\varepsilon^2)][1 - \frac{1}{2}c^2\varepsilon z^2]}{[1 + O(\varepsilon^2)]}u = O(e^{-1/\varepsilon})$$

$$\varepsilon L_z[v] + [1 + O(\varepsilon^2)]u = O(e^{-1/\varepsilon})$$

Up to terms of order ε^2 or smaller, we have $(u, v) \sim (\tilde{u}, \tilde{v})$ with

$$\begin{aligned} \varepsilon L_z[\tilde{u}] - \tilde{v} + 2(1 + \alpha_1\varepsilon)(1 - \frac{1}{2}\varepsilon c^2 z^2)\tilde{u} &= 0 \\ \varepsilon L_z[\tilde{v}] - \tilde{u} &= 0 \end{aligned} \quad (5.8)$$

We seek an asymptotic solution of (5.9) in the form

$$\begin{pmatrix} \tilde{u} \\ \tilde{v} \end{pmatrix} \sim e^{iz/\sqrt{\varepsilon}} \sum_{n=0}^{\infty} \begin{pmatrix} U_n \\ V_n \end{pmatrix} \varepsilon^{n/2} \quad (5.9)$$

It is not difficult to verify that the ODE for \tilde{u} and \tilde{v} are satisfied identically in ε to terms of order ε if

$$\begin{aligned} U_0 &= V_0, & U_1 &= V_1 - 2iV_0' - \frac{i}{z}V_0 \\ U_2 &= V_2 - 2iV_1' - \frac{i}{z}V_1 + (\frac{3}{4z^2} + \frac{\alpha_1}{2} - z^2)V_0 \end{aligned} \quad (5.10)$$

and

$$V_0'' + \frac{1}{z}V_0' - (\frac{1}{4z^2} - \frac{\alpha_1}{2} + z^2)V_0 = 0 \quad (5.11)$$

with $(\quad)' = d(\quad)/dz$. The ODE (5.12) for V_0 may be transformed into

$$w'' + (\frac{\alpha_1}{2} - z^2)w = 0 \quad (5.12)$$

where $w = \sqrt{z}V_0$. The solutions for (5.13) are parabolic cylinder functions $D_\nu(t)$ and $D_{-\nu-1}(it)$ where $\nu = (\alpha_1 - 2)/4$ and $t = \sqrt{2}z$ [13]. Altogether, we have the following asymptotic solution for \tilde{u} and \tilde{v} :

$$\bar{u} \sim \bar{v} \sim \frac{e^{iz/\sqrt{\varepsilon}}}{\sqrt{z}} \left[c_1 D_{-\frac{1}{2} + \frac{\alpha_1}{4}}(\sqrt{2z}) + d_1 D_{-\frac{1}{2} - \frac{\alpha_1}{4}}(i\sqrt{2z}) \right] [1 + O(\sqrt{\varepsilon})] \quad (5.13)$$

+complex conjugate of the preceding expression.

For large values of the argument, we have the following asymptotic behavior for $D_\nu(t)$ and $D_{-\nu-1}(it)$:

$$\begin{aligned} D_\nu(t) &\sim t^\nu e^{-t^2/4} \sum_{n=0}^{\infty} (-1)^n \gamma_n t^{-2n}, \\ D_{-\nu-1}(it) &\sim (it)^{-\nu-1} e^{t^2/4} \sum_{n=0}^{\infty} \gamma_n t^{-2n} \end{aligned} \quad (5.14)$$

for $t \rightarrow \infty$, $|\arg(t)| < 3\pi/4$ with $\gamma_0 = 1$, $\gamma_1 = \nu(\nu-1)/2$, etc. They show that matching of (\bar{u}, \bar{v}) and (u, v) as given by (5.7) may be accomplished by taking

$$c_1 = \frac{2^{-(\alpha_1+6)}/8}{i^{3/2}\varepsilon^{-(\alpha_1-4)}/8} c_0, \quad d_1 = \frac{2^{(\alpha_1-6)}/8_i \alpha_1/4}{\varepsilon^{(\alpha_1+4)}/8} d_0^* \quad (5.15)$$

For small values of the argument, we have from the Taylor series representation of the parabolic cylinder functions

$$D_\nu(t) = \frac{\sqrt{2^\nu \pi}}{\Gamma(\frac{1}{2} - \frac{1}{2}\nu)} \left[1 - \frac{\Gamma(\frac{1}{2} - \frac{1}{2}\nu)}{\Gamma(\frac{-1}{2}\nu)} \sqrt{2}t + O(t^2) \right] \quad (5.16)$$

which allows to match the parabolic cylinder function solution with the Bessel function solution in an intermediate (overlapping) region of validity. The matching is accomplished to order ε with

$$\begin{aligned} c_{1r} + \frac{\Gamma(\frac{3}{4} - \frac{\alpha_1}{8})}{2^{\alpha_1/4} \Gamma(\frac{3}{4} + \frac{\alpha_1}{8})} d_{1r} &= c_{1i} + \frac{\Gamma(\frac{3}{4} - \frac{\alpha_1}{8})}{2^{\alpha_1/4} \Gamma(\frac{3}{4} + \frac{\alpha_1}{8})} d_{1i} = -\frac{\varepsilon^{1/4} \Gamma(\frac{3}{4} - \frac{\alpha_1}{8})}{\pi 2^{(\alpha_1+6)}/8} a_0 \\ -c_{1r} + \frac{2^{\alpha_1/4} \Gamma(\frac{1}{4} - \frac{\alpha_1}{8})}{\Gamma(\frac{1}{4} + \frac{\alpha_1}{8})} d_{1i} &= c_{1i} + \frac{2^{\alpha_1/4} \Gamma(\frac{1}{4} - \frac{\alpha_1}{8})}{\Gamma(\frac{1}{4} + \frac{\alpha_1}{8})} d_{1r} = \frac{\varepsilon^{-1/4} \Gamma(\frac{1}{4} - \frac{\alpha_1}{8})}{\pi 2^{(\alpha_1+14)}/8} \bar{b}_0 \end{aligned} \quad (5.17)$$

where (c_{1r}, d_{1r}) and (c_{1i}, d_{1i}) are the real and imaginary parts of (c_1, d_1) respectively, and $b_0 = \bar{b}_0 \sqrt{\varepsilon}$.

5.4 Matching and Solutions of Eigenvalue Problem

The four conditions (5.17) determine the two complex constants c_1 and d_1 in terms of the two real constants a_0 and \bar{b}_0 . It follows from (5.17)

X 7
X 5

that the two complex constants c_0 and d_0 , which appear in the WKB solution, are also determined in terms of the two real constants a_0 and b_0 . Finally, these two unknown real constants must be chosen so that clamped edge conditions (4.4') are satisfied by the WKB solution (5.7). The two clamped edge conditions at $x = 1$ are two homogeneous linear equations for a_0 and b_0 . For a nontrivial solution, the determinant of the 2×2 coefficient matrix must vanish. We omit the lengthy expression for the determinant obtained from this tedious but straightforward solution procedure, and merely report that, except for exponentially small terms, the determinant vanishes only if $\alpha_1 = 0$. Therefore, the eigenvalues of the linearized problem (4.2')-(4.4') is given by $\bar{\kappa} = \kappa = 1 + O(\varepsilon^2)$ (for $c = 2$). The eigenfunctions are given

- by (5.7) with $\alpha_1 = 0$ away from the apex,
- by (5.5) in the neighborhood of the apex, and
- by (5.14) with $\alpha_1 = 0$ for an intermediate region.

The complex constants c_0, d_0, c_1 and d_1 are determined in terms of the two real constants a_0 and $b_0 \equiv \bar{b}_0 \sqrt{\varepsilon}$ by (5.16) and (5.18). The constant a_0 is determined in terms of b_0 by either one of the clamped edge conditions. The result $\alpha_1 = 0$ is consistent with the COLSYS solutions given in Table (2). To determine the $O(\varepsilon^2)$ correction for the eigenvalues, we will need higher order terms in the various asymptotic expansions including the basic branch solution.

6. Concluding Remarks

By the asymptotic analysis of sections (3)-(5), we have established that, for $c = 2$ and $\varepsilon \ll 1$, branching from the basic solution (of section (3) or (4)) is not possible for p_0 not nearly p_s . Branching when $(\bar{\kappa} = \kappa = [1 + O(\varepsilon^2)])$ remains a possibility but requires a separate analysis. With the smaller size dimple shrinking to zero as κ tends to 1-, it would seem that the lowest mode axisymmetric bifurcation is to the dimple branch. In any event, axisymmetric bifurcation first occurs at a rather high pressure magnitude, namely $p_0 \cong p_s$ for $c = 2$ and $\varepsilon \ll 1$, compared to the critical magnitude p_{cr} for which the appearance of a dimple is possible; the linear buckling load is therefore not an important design consideration (unless polar dimpling is the preferred mode) compared to asymmetric bifurcation, say. For this reason, we did not attempt to describe in more details the eigenvalues and eigenfunctions than we did in sections (4) and (5) or the branching analysis for $\kappa = O(1)$. On

the other hand, the analysis of post-buckling behavior and imperfection sensitivity should be of interest.

Notes

1. Within the framework of a shallow shell theory, there is no distinction between normal and axial loads.

References

- [1] K.O. Friedrich, On the minimum buckling load for spherical shells , *Th. von Karman Anniversary Volume*, Caltech (Pasadena), 1941, 258-272.
- [2] D.G. Ashwell, On the large deflexion of a spherical shell with an inward point load , *Proc. IUTAM Symp. on Thin Shells (Delft)*, Ed. W.T. Koiter, North-Holand, Amsterdam, 1960, 43-63.
- [3] C.V. Ranjan and C.R. Steele, Large deflection of deep spherical shells under concentrated load , *Proc. AIAA/ASME 18th Structures, Struc. Dynamics and Materials Conf.* (San Diego), 1977, 269-278.
- [4] F.Y.M. Wan, The dimpling of spherical caps , *Mechanics Today 5* (The Eric Reissner Anniversary Volume), 1980, 495-508.
- [5] F.Y.M. Wan, Polar dimpling of complete spherical shells , *Proc. (3rd) IUTAM Sym. on Thin Shells (Tibilisi): Theory of Shells*, Ed. W.T. Koiter & G.K. Mikhailov, North-Holland, 1980, 589-605.
- [6] F.Y.M. Wan & U. Ascher, Horizontal and flatpoints in shallow shell dimpling , *Proc. BAIL I Conf.* Ed. J. Miller, Boole Press, Dublin, 1980, 659-679.
- [7] L.A. Taber, Large deflection of a fluid-filled spherical shell under a point load , *J. Appl. Mech.*, **49**, 1982, 121-128.
- [8] F.Y.M. Wan, Shallow caps with a localized pressure distribution centered at the apex , *Proc. EUROMECH Colloq. (No. 165) on Flexible Shells (Munich)*, Ed. E. Axelrad & F. Emmerling, Springer-Verlag, Berlin-New York-Heidelberg, 1984, 124-145.
- [9] D.F. Parker & F.Y.M. Wan, Finite polar dimpling of shallow caps under sub-buckling pressure loading , *SIAM J. of Appl. Math.*, **44** 1984, 301-326.
- [10] E. Reissner, On axisymmetric deformations of thin shells of revolution , *Proc. Symp. in Appl. Math.*, Vol.III, Amer. Math. Soc., Providence, 1950, 27-52.
- [11] E. Reissner, Symmetric bending of shallow shells of revolution , *J. Math Mech.*, **1**, 1958, 121-140.

- [12] U. Ascher, J. Christiansen and R.D. Russell, A collocation solver for mixed order systems of boundary value problems , *Math. Comp.*, **33**, 1979, 659-679.
- [13] U. Ascher, R.M.M. Mattheij & R.D. Russell, *Numerical Solutions of Boundary Value Problems for Ordinary Differential Equations*, (Classics in Applied Mathematics, vol. 13) SIAM Publications, Philadelphia, 1995.
- [14] M. Abramowitz & I.A. Stegun, *Handbook of Mathematical Functions*, AMS No. 55 of National Bureau of Standards, 1964, U.S. Government Printing Office, Washington D.C.
- [15] C.G. Lange & G.A. Kriegsmann, The axisymmetric branching behavior of complete spherical shells , *Quart. Appl. Math.*, **39**, 1981, 145-178.